Two-Photon Absorption Properties of Self-Assemblies of Butadiyne-Linked Bis(Imidazolylporphyrin)

Kazuya Ogawa,[†] Atsushi Ohashi,[†] Yoshiaki Kobuke,*[,†] Kenji Kamada,[‡] and Koji Ohta[‡]

Graduate School of Materials Science, Nara Institute of Science and Technology, 8916-5 Takayama, Ikoma, Nara 630-0101, Japan, and Photonics Research Institute, National Institute of Advanced Industrial Science and Technology, 1-8-31 Midorigaoka, Ikeda, Osaka 563-8577, Japan

Received: August 9, 2005; In Final Form: September 22, 2005

Supramolecular porphyrin self-assemblies have been prepared from butadiyne-linked bis(imidazolylporphyrin) by complementary coordination of imidazole to zinc, and their two-photon absorption (2PA) and higher-order nonlinear absorption properties were investigated over femtosecond time scales using an open-aperture Z-scan method. The self-assembled porphyrin dimer of the conjugated monozinc bisporphyrin **7D** was shown to have a large 2PA cross section (7.6×10^3 GM, where 1 GM $= 10^{-50}$ cm^4 s molecule^{-1} photon^{-1}) at 887 nm. By comparison of this result with that for a meso−meso-linked porphyrin array without the butadiyne connection (3.7×10^2 GM at 964 nm), it was demonstrated that the predominant factor in this significant enhancement of the cross section was the expansion of porphyrin−porphyrin π-conjugation. Self-coordination and monozinc metalation were also found to be contributing factors. Furthermore, a novel self-assembled porphyrin polymer **8P** consisting of a biszinc complex with a mean molecular weight of $M_n = 1.5 \times 10^5$ Da was shown to exhibit an extraordinarily large two-photon absorption cross section (4.4×10^5 GM at 873 nm). Nanosecond Z-scan experiments for **7D** and **8P** were also undertaken and resulted in the measurement of large effective 2PA cross sections, including the excited-state absorption (2.1×10^5 GM for **7D** and 2.2×10^7 GM for **8P**, respectively). Finally, three-photon absorption was observed by femtosecond Z-scan experiments at 1188 nm (7.1×10^{-89} m^6 s^2) and 1282 nm (1.8×10^{-89} m^6 s^2), an observation which is the first of its kind in porphyrin chemistry.

Introduction

In recent years, much attention has been focused on materials that exhibit two-photon absorption (2PA) because of their potential applications in a range of applications including two-photon photodynamic therapy (2PA-PDT),[1] three-dimensional (3-D) optical memory,[2] optical power limiting,[3] 3-D microfabrication,[4] and fluorescence microscopy.[5]

2PA processes are nonlinear optical processes related to the imaginary part of the third-order susceptibility.[6] Since 2PA is proportional to the square of the laser light power, the efficiency is largest at the spot where the laser beam is most strongly focused. In other words, the process tends to be strongly localized. One important potential application of this property would be in the treatment of cancer. Porphyrin derivatives are presently used as photosensitizers during one-photon PDT in cancer treatment; irradiated porphyrins move from the S1 state (which can be generated from the S2 state by internal conversion) into an excited triplet state, producing singlet oxygen in a highly efficient way.[7] Cancer cells are thus flooded with singlet oxygen and are destroyed. However, the efficiency of the treatment is limited by the poor permeability of the surface tissue to the visible light used to irradiate the porphyrins. A more efficient method would be to use two photons in the near-infrared (NIR) range, which corresponds to an "optical window" for biological tissue.[8] These photons readily penetrate the surface and may then be absorbed simultaneously to excite the molecule. Thus, 2PA-PDT may allow the localized treatment of cancer even at significant depths below the surface tissue.

Another important application of 2PA processes is in the production of memory devices. Current optical memory devices, which use a heat mode recording method to store information two-dimensionally, have a storage density limit of approximately gigabits per square centimeter. The creation of 3-D optical memory devices that use 2PA materials and a photon mode recording method is expected to significantly increase the potential storage density to as high as terabits of information per cubic centimeter.[9] This information density is the equivalent of $\sim 1 \times 10^6$ floppy disks, and the use of a 2PA material would also result in an ultrafast access speed.

It has been proposed that a molecular design that would result in a large 2PA cross section ($\sigma^{(2)}$) would be composed of sets of terminal donor/acceptors interspersed with a π-conjugation system in either a symmetrical (D−π−D or A−π−A)[10] or asymmetrical (D−π−A)[11] arrangement. Porphyrins and phthalocyanines are thus very likely candidates for 2PA materials because of their highly conjugated large π-system. However, monomeric porphyrins without donor/acceptor groups have shown only small $\sigma^{(2)}$ values (less than 10^2 GM where 1 GM $= 10^{-50}$ cm^4 s molecule^{-1} photon^{-1}) when measured using femtosecond pulse lasers.[12]

We have previously reported that a zinc complex of *meso*-1-methylimidazolylporphyrin (**1**) can be used in the formation of a stable slipped cofacial dimer **2D** through complementary coordination of the imidazolyl to penta-coordinating zinc in a non-coordinating solvent.[13a] This methodology has been devel-

* Author to whom correspondence should be addressed. E-mail: kobuke@ms.naist.jp.
[†] Nara Institute of Science and Technology
[‡] National Institute of Advanced Industrial Science and Technology

10.1021/jp054444z CCC: $30.25
Published on Web 10/22/2005

SCHEME 1: Formation of Self-Assembled Dimer and Giant Porphyrin Array by Complementary Coordination of Imidazole to Zinc

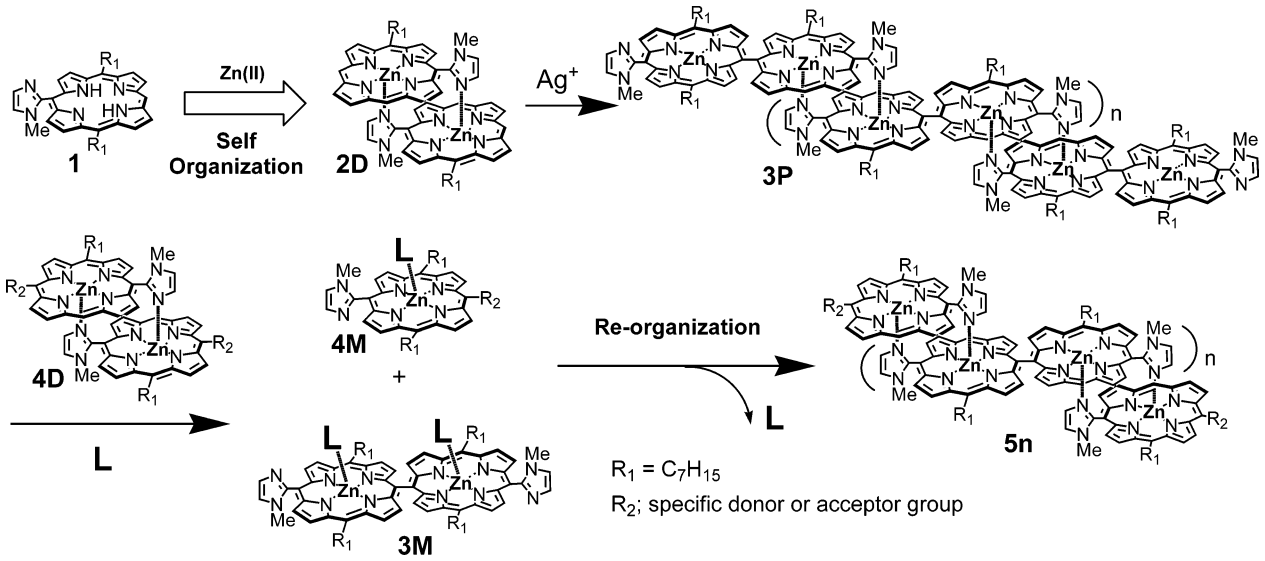

CHART 1: Compounds Used in This Study

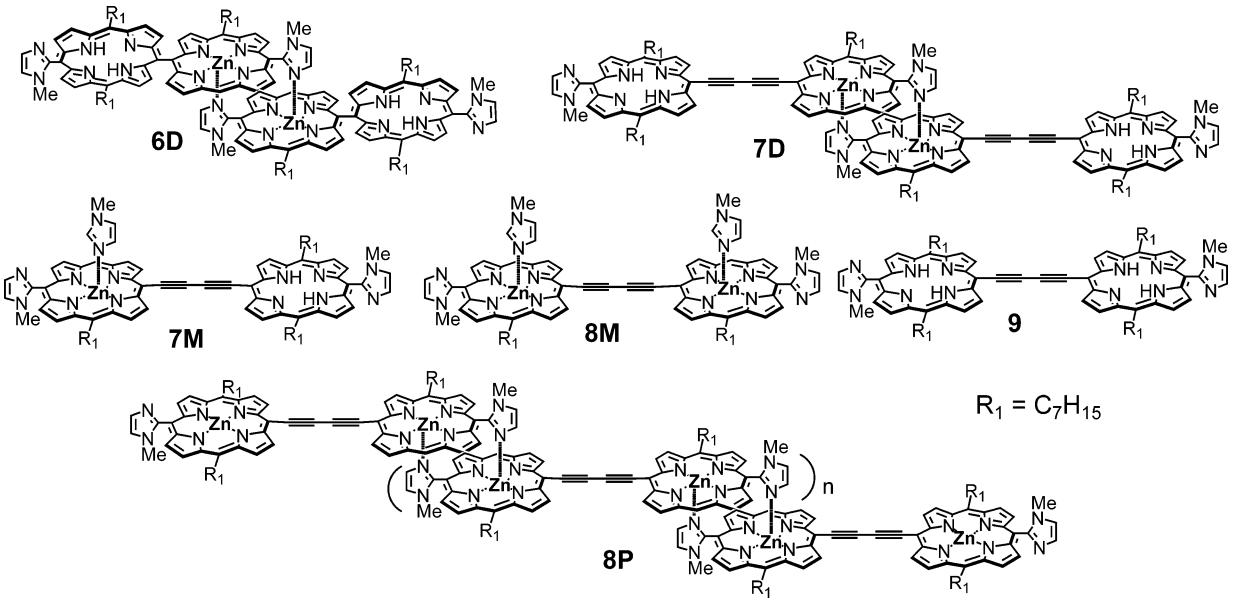

oped to produce unique supramolecular porphyrin systems.[13] A giant supramolecular porphyrin array **3P** of up to 8×10^2 porphyrin units was obtained in a dilute $CHCl_3$ solution by linking two imidazolylporphyrin units directly at the meso positions.[13b] The polymeric structure could be cleaved by introducing coordinating solvents such as MeOH or pyridine and regenerated again by eliminating such solvents. When this reorganization (i.e., the cleavage−reorganization cycle) was undertaken in the presence of poly(porphyrin) **3P** and another imidazolylporphyrinatozinc dimer **4D**, the resulting product **5n** was composed of oligomers **3P** of much smaller numbers of n terminated with **4M** terminals. In this way, the reorganization procedure led to the development of an efficient method for introducing appropriate donor and/or acceptor groups at the molecular terminals of the array in the form of R_2-appended imidazolyl zinc porphyrin. The use of freebase porphyrin as an acceptor R_2 resulted in large enhancements of the real part of the molecular second hyperpolarizability compared with self-assemblies having no acceptor group.[13c] However, no nonlinear absorption was observed using femtosecond optical Kerr effect (OKE) measurements at the off-resonant wavelength (800 nm), even when increased laser power was used.

To extend the use of this supramolecular porphyrin system to 2PA materials (i.e., to obtain a large 2PA cross section), we designed a novel porphyrin assembly **7D**[13e] according to the general strategy outlined above. First, π-conjugation between two porphyrins was expanded by using a butadiyne connection that permitted a coplanar orientation of the molecules. This is necessary because the orthogonal orientation of the meso−meso-linked bisporphyrins shown in Scheme 1 prevents the desired porphyrin−porphyrin π-conjugation. Recently, it was found that the butadiyne linkage in the A−π−A structure for a small organic molecule can result in large $\sigma^{(2)}$ values.[13e,14a,b] The conjugated porphyrin arrays, covalently linked by butadiyne[15] and ethyne linkages,[16] are assumed to be converted to cumulenic structures upon photoexcitation. This may make the absorption of the second photon favorable[15f] and encourage nonlinear optical behavior. Second, free base porphyrins were introduced at both terminals of the assembly to promote molecular polarization in an A−π−D−π−A form.

SCHEME 2: Synthetic Route of Butadiyne-Linked Bisporphyrin 9 and Self-Assemblies

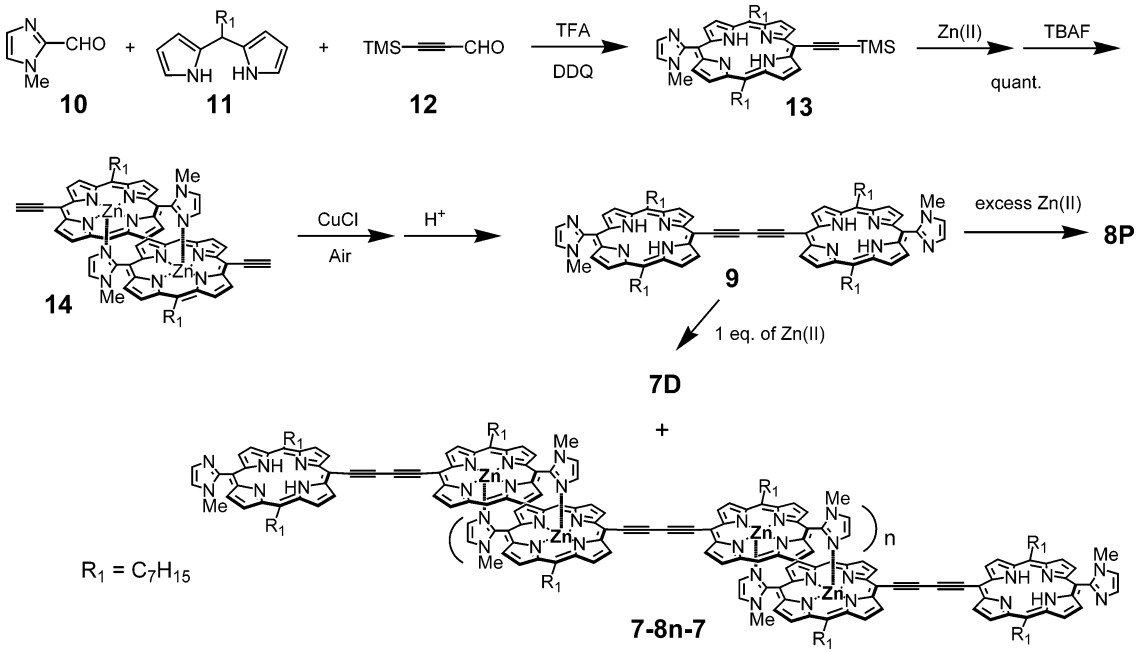

In this study, the 2PA cross section of self-assembled conjugated porphyrin **7D** consisting of two monozinc complexes of bisimidazolylporphyrin was measured using a femtosecond Z-scan technique. To elucidate the effect of the butadiyne linker, the cross section of self-assembled porphyrin **6D** without a butadiyne unit was also measured. Next, to investigate the effects of the complementary coordination of imidazolyl to zinc and the impact that the introduction of monozinc has on the enhancement of the 2PA cross section, bisporphyrin units of monozinc complex **7M**, bis(free base) **9**, and biszinc complex **8M** generated by the addition of 1-methylimidazole were measured. At the same time, we took advantage of the opportunity to examine the $\sigma^{(2)}$ value of an interesting long linear polymer **8P**, which is formed spontaneously through successive complementary coordination of imidazolyl to zinc. Finally, the nanosecond 2PA properties of **7D** and **8P** were investigated. This was part of our broader interest in the possible application of the substance in 2PA-PDT. We considered that the nanosecond Nd:YAG−optical parametric oscillator (OPO) system may have advantages for use in 2PA-PDT because the apparatus is relatively convenient, inexpensive, and readily available in medical institutions now providing one-photon PDT.

Results and Discussion

Synthesis of 9. The synthetic route of conjugated bis(imidazolylporphyrin) **9** bridged by a butadiyne linkage is summarized in Scheme 2. This synthesis has been reported in a preliminary communication.[13e] The starting material (*n*-heptyldipyrromethane (**11**)) was prepared from 1-octanal and 40 equiv of pyrrole with trifluoroacetic acid (TFA), in accordance with the previous report.[17] The reaction of **11** with 1-methyl-2-formylimidazole (**10**) and trimethylsilylpropynal (**12**) using TFA as a catalyst, followed by *p*-chloranil oxidation, resulted in a crude mixture. Purification by SiO_2 column chromatography allowed for the extraction of free base porphyrin **13**, which was characterized using matrix-assisted laser desorption ionization time of flight mass spectrometry (MALDI-TOF MS) and ^{1}H and ^{13}C NMR. The zinc insertion and deprotection of the trimethylsilyl (TMS) group quantitatively demonstrated the presence of the complementary dimer of zinc porphyrin **14** without the need for further purification. The conjugated bis(imidazolylporphyrin) **9** was synthesized by a homocoupling reaction of **14** under the Glaser coupling condition[18] using CuCl and pyridine in the presence of oxygen at room temperature, followed by a demetalation step with TsOH for the purposes of purification. Pure **9** was obtained via SiO_2 column chromatography and preparative gel permeation chromatography (GPC) with an isolated yield of 15%. It was identified through ^{1}H NMR, analytical gel permeation chromatography (GPC)−high-performance liquid chromatography (HPLC), MALDI-TOF MS, and thin-layer chromatography. The UV/vis absorption spectrum of **9** is shown in Figure 1 (dashed line) along with that of polymer **8P** (solid line). The Q-band of **9** was observed at around 715 nm. It is red-shifted by 48 nm compared with the Q-band position of the monomeric free base **13** (667 nm), which suggests the expansion of π-conjugation between the two porphyrins.[15]

Formation of Self-Assembly. *Tetramer 7D.* To investigate the effect of π-conjugation between the porphyrins on the substance's 2PA level, discrete tetrameric porphyrin assemblies **6D** and **7D** were prepared in the hope of enhancing molecular polarization. The construction of each of these was based on the self-coordination of two monozinc complexes. The preparation of self-assembled tetramer **6D** has been reported in an

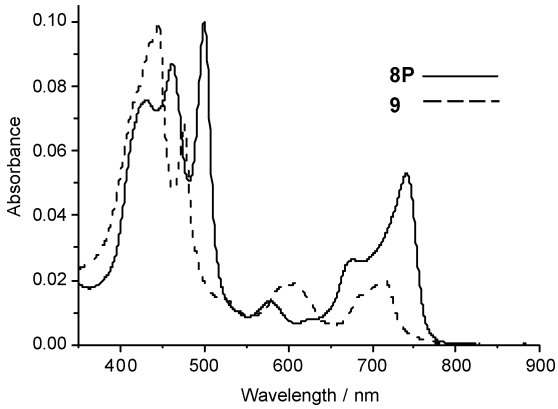

Figure 1. One-photon absorption spectra of **8P** (solid line) and **9** (dashed line) in $CHCl_3$.

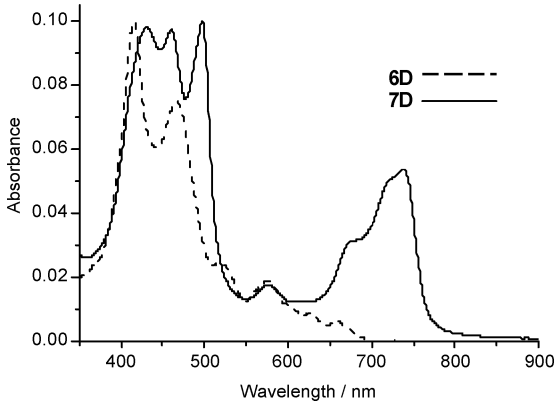

Figure 2. One-photon absorption spectra of **6D** (dashed line) and **7D** (solid line) in $CHCl_3$.

SCHEME 3: Preparation of Monomeric Species for 2PA Measurements

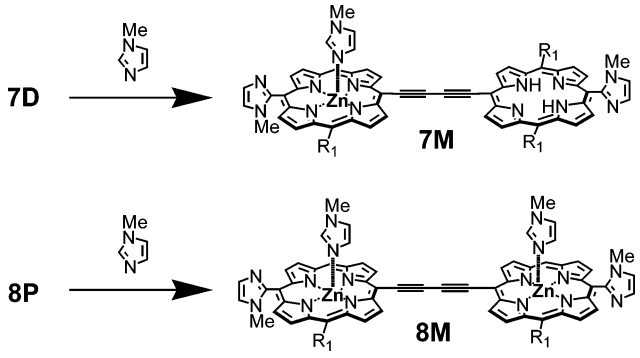

earlier communication.[13c] During the preparation of the **7D**, a reaction with 1 equiv of zinc acetate resulted in a mixture of **9**, **7D**, and biszinc complexes that existed as oligomeric mixtures terminated by the monozinc complex **7**−**8n**−**7** in chloroform (Scheme 2). The target **7D** was isolated by a preparative recycling GPC process eluting with chloroform. The UV/vis absorption spectra of **7D** and meso−meso-linked **6D** are shown in Figure 2. The Q-band of **7D** was red-shifted to ∼740 nm compared to that of **6D** (660 nm). Its intensity was also significantly increased, a fact which may be attributable to the expansion of the π-conjugation due to the presence of the butadiyne linkage.

*Polymer **8P***. The reaction of bis(free base) **9** with excess quantities of zinc acetate resulted in the production of a biszinc complex, which allowed the formation of the one-dimensionally propagated polymer **8P** through the successive complementary coordination of imidazolyl to zinc. The UV/vis absorption spectrum of **8P** is shown above in Figure 1 (solid line). A characteristic feature of this spectrum is the fact that the Q-band of polymer **8P** appears at 741 nm. That is, it is red-shifted from the 728 nm Q-band position that appears in the spectrum of monomeric biszinc bisporphyrin **8M** coordinated by 1-methylimidazole (Scheme 3). This shift is a result of exciton interactions in the head-to-tail arrangement along the direction of the linear assembly. The molecular weight of polymer **8P** was analyzed using GPC with a column having an exclusion limit of 5×10^5 Da by elution with chloroform. Figure 3 shows the GPC chart of **8P** monitored at 410 nm by a UV/vis photodiode array. The figure also includes a GPC chart for certain standard polystyrene mixtures. The absorption spectra of **8P** at different retention times between 7 and 12 min were identical. The polymer **8P** started to be eluted even before the retention time of the standard molecular weight ($M_w = 5.5 \times 10^5$ Da), and the distribution maximum appeared around $M_w = 1.5 \times 10^5$ Da, which corresponds to ca. 110 bis(imidazolylporphyrin) units (where the M_w of one unit corresponds to 1346.40 Da). The mean molecular weights, M_w and M_n, were estimated by comparing the data with those of polystyrene standards. They were found to be $\sim 2.2 \times 10^5$ and $\sim 1.5 \times 10^5$ Da, respectively, which results in a polydispersity index of $M_w/M_n = 1.5$ (Experimental Section). A molecular weight of this size is a result of the successive complementary coordination of imidazole to Zn. Despite a polymeric structure and a large molecular weight, **8P** is soluble in chloroform, tetrahydrofuran (THF), and toluene but insoluble in methanol, ethyl acetate, and hexane.

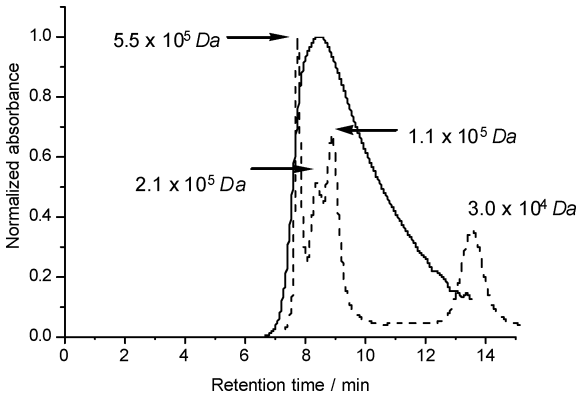

Figure 3. Gel permeation chromatograms of **8P** (solid line) and a standard polystyrene mixture (dashed line) eluted by chloroform containing 0.5% ethanol. The exclusion limit of the column is 5×10^5 Da.

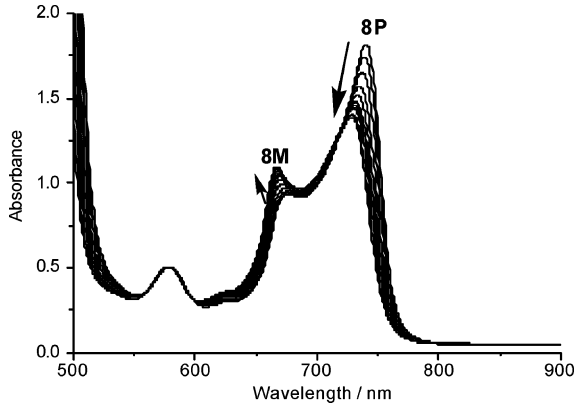

Figure 4. Change of one-photon absorption spectra by titrating 1-methylimidazole into a chloroform solution of polymer **8P**.

Preparation of Monomeric species. To investigate the effect both of the complementary coordination of imidazolyl to zinc and of monozinc metalation on the substances' tendency to undergo 2PA, monomeric units of monozinc complex **7M** and biszinc complex **8M** were prepared. As has already been pointed out, the complementary coordination of imidazolyl to zinc can be dissociated into the ligand-coordinated monomer by adding a competing ligand such as methanol, pyridine, or 1-methylimidazole.[13b,d] The amount of 1-methylimidazole required to completely dissociate the polymer **8P** into **8M** was determined by titration experiments. As shown below in Figure 4, the Q-bands of **8P** appeared at 677 and 741 nm. The bands were blue-shifted after a titration of 1-methylimidazole into 0.5 mM chloroform solution (0.5 mL) of **8P** (calculated per biszinc unit) because of the cleavage of the complementary coordination. The changes in the absorption spectra ceased once 3000 equiv of 1-methylimidazole (∼1.5 M) had been added, indicating complete dissociation of the **8P** to the monomer **8M**. The 3000 equiv of

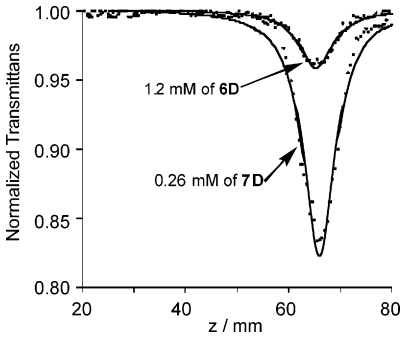

Figure 5. Typical open-aperture Z-scan traces (dot) of **6D** and **7D** measured using femtosecond pulses at 964 nm with a pulse energy of 0.31 μJ corresponding to $I_0 = 1.2 \times 10^{15}$ W m^{-2} with theoretical fitting curves (solid).

1-methylimidazole were also sufficient to dissociate **7D** into **7M**. Therefore, the chloroform solution containing 1.5 M 1-methylimidazole was used during the 2PA measurements of **7M** and **8M**.

Two-Photon Absorption Properties. *Effect of the Expansion of π-Conjugation between Porphyrins on 2PA.* As a first step in the investigation of the effect of the expansion of the π-conjugation between bis(imidazolylporphyrin) on 2PA processes, two self-assemblies **6D** and **7D** were examined. The butadiyne linkage in **7D** allows a coplanar orientation between the bis(imidazolylporphyrin)s, leading to an increase in π-conjugation, whereas two porphyrins directly linked at meso-positions in self-assembly **6D** are almost orthogonal to each other and thus prevent porphyrin−porphyrin π-conjugation.[19] The 2PA cross sections were measured with open-aperture Z-scan experiments[20] at wavelengths from 817 to 1282 nm, using a femtosecond optical parametric amplifier. The open-aperture Z-scan technique is an experimental method that detects nonlinear absorption by scanning the sample around the focal point along the direction of laser beam. The nonlinear absorption is observed most strongly near the focal point, where the intensity of the incident light is a maximum. The use of a femtosecond laser for the Z-scan measurements minimizes the contribution of excited-state absorption (ESA) processes to the signal, which has been found to make a considerable difference to the outcome of picosecond and nanosecond pulse measurements.[21] Both of the self-assemblies show significant one-photon absorption in the 400−500 nm range, which corresponds to the Soret band (S_2 state). In contrast, only very weak and no absorption are observed at longer wavelengths over 800 nm in **7D** and **6D**, respectively. This is because in the 800−1000 nm region it is expected that two photons will need to be absorbed simultaneously to promote the molecules to the S_2 state. The process will require high-intensity laser pulses.

Figure 5 shows typical Z-scan traces for **6D** and **7D** in chloroform (dotted trace) and theoretically fitted curves (solid line). These particular sets of data were measured with a pulse energy of 0.31 μJ (corresponding to an on-axis peak intensity at the focal position of $I_0 = 1.2 \times 10^{15}$ W m^{-2}). In this figure, the normalized transmittance is plotted as a function of the sample position, z. A control experiment with pure chloroform showed a flat Z-scan trace, indicating that there is no nonlinear absorption due to the solvent up to a maximum incident intensity of $I_0 = 2.2 \times 10^{15}$ W m^{-2} (the upper power limit used in this study). However, self-assembly **7D** showed a significant drop in the intensity of the light transmitted through the sample due to the effects of nonlinear absorption.

The $\sigma^{(2)}$ value was calculated from the two-photon absorbance q_0 obtained by fitting a theoretical curve to the observed open-aperture traces. The curve fit was based on the theoretical expression for the transmittance[14c,d]

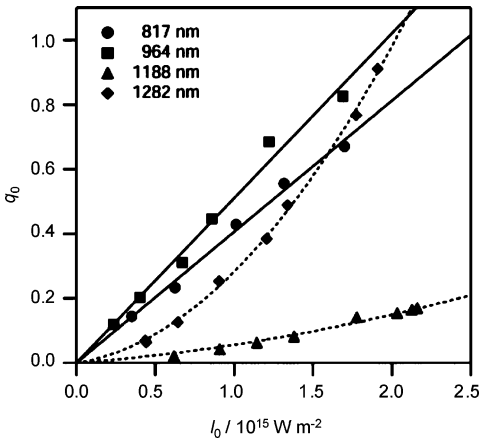

Figure 6. Plots of the two-photon absorbance q_0 versus on-axis peak intensity at the focal position I_0 for **7D** using femtosecond pulses at different wavelengths with linear (solid line) and quadratic (dashed line) curve fits. Concentrations of the sample solutions were 0.26 mM for 817 and 964 nm, 0.24 mM for 1188 nm, and 1.5 mM for 1282 nm.

$$T(\zeta) = \frac{(1-R)^2\, e^{(-\alpha^{(1)}L)}}{\sqrt{\pi} q(\zeta)} \int_{-\infty}^{\infty} \ln[1 + q(\zeta)\, e^{(-x^2)}]\, dx \quad (1)$$

$$q(\zeta) = \frac{q_0}{1+\zeta^2} \quad (2)$$

Equation 1 describes the normalized transmittance of a sample that exhibits only 2PA for a Gaussian-pulsed Gaussian beam, where ζ is the normalized Z-position ($\zeta = (z - z_0)/z_R$), and z_0 and z_R are the focal position and the Rayleigh range, respectively. $T(\zeta)$ is normalized to unity at a position far from the focal point, i.e., $T(\zeta \rightarrow \pm\infty) = 1$. $\alpha^{(1)}$ is the linear (one-photon) absorption coefficient, R is the Fresnel reflectance at the cuvette cell walls, and L denotes the path length of the sample. The two-photon absorbance q_0 is defined as

$$q_0 = \alpha^{(2)}(1-R) I_0 L_{\text{eff}} \quad (3)$$

where $\alpha^{(2)}$ is the 2PA coefficient, L_{eff} denotes the effective path length defined as $L_{\text{eff}} = [1 - \exp(-\alpha^{(1)}L)]/\alpha^{(1)}$, and I_0 is the on-axis peak intensity at the focal position as mentioned above. Since **6D** showed no one-photon absorption at over 800 nm, L_{eff} reduced to L. However, weak one-photon absorption was observed up to 900 nm for **7D**, so the 2PA data at those wavelengths was treated using L_{eff}. No sign of saturable absorption was found at the measured wavelengths. Figure 6 shows plots of the two-photon absorbance q_0 against I_0 for **7D** at different wavelengths. Equation 3 predicts a linear relationship between q_0 and I_0 for the 2PA process. This behavior was in fact observed for all compounds at wavelengths shorter than ~1188 nm, which demonstrates that 2PA is the dominant process at these wavelengths. In contrast, parabolic behavior was observed for wavelengths longer than 1180 nm, suggesting that higher-order multiphoton absorption, in preference to 2PA, is occurring in this regime. The significance of this will be discussed below.

The value of $\alpha^{(2)}$ is the slope of the q_0 versus I_0 plot. From this, the value of $\sigma^{(2)}$ could be found since

$$\sigma^{(2)} = \frac{h\omega\alpha^{(2)}}{N} \quad (4)$$

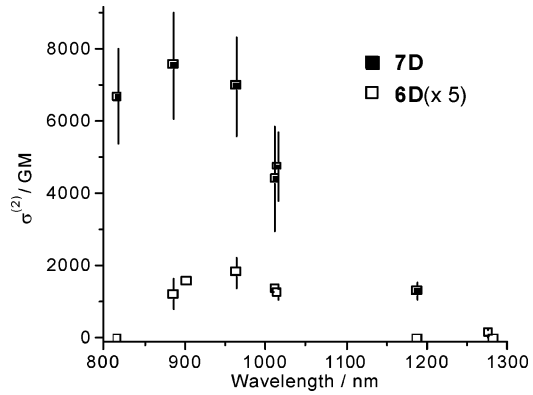

Figure 7. 2PA spectra of **6D** and **7D** measured using femtosecond pulses in $CHCl_3$.

TABLE 1: 2PA Cross Section Values ($\sigma^{(2)}$) of Porphyrins[a]

sample	$\sigma^{(2)}$/GM (per dimer unit)	pulse width	wavelength/nm
6D	3.7×10^2 (1.8×10^2)	120 fs	964
7D	7.6×10^3 (3.8×10^3)	120 fs	887
	2.1×10^5 (1.1×10^5)	5 ns	890
7M	1.8×10^3 (1.8×10^3)	120 fs	873
8M	1.2×10^3 (1.2×10^3)	120 fs	873
8P	4.4×10^5 (4.0×10^3)	120 fs	873
	2.2×10^7 (2.0×10^5)	5 ns	890
9	1.0×10^3 (1.0×10^3)	120 fs	873

[a] Femtosecond data were obtained in chloroform for **6D**, **7D**, and **8P** and chloroform containing 1.5 M 1-methylimidazole for **7M**, **8M**, and **9**. Nanosecond data for **7D** and **8P** were measured in toluene.

where N denotes the number density of in the sample molecules and $h\omega$ is the photon energy of the incident light.

The $\sigma^{(2)}$ values for **6D** and **7D** at different wavelengths in $CHCl_3$ are shown in Figure 7. The maximum $\sigma^{(2)}$ values in each case were estimated to be $(3.7 \pm 0.8) \times 10^2$ GM ((1.86 ± 0.4) $\times 10^2$ per unit) at 964 nm and $(7.6 \pm 1.5) \times 10^3$ GM ((3.8 ± 0.74) $\times 10^3$ per unit) at 887 nm (Table 1). Note that the maximum $\sigma^{(2)}$ value for **7D** is almost 20 times larger than that for **6D**. This result shows that the expansion of π-conjugation between porphyrin units, which was made possible by the introduction of the butadiyne linkage, is the most important factor in the enhancement of the $\sigma^{(2)}$ value for this substance. The value (7.6×10^3 GM) belongs to the largest class of organic compounds measured in the femtosecond time scale.[12,14,15f,g,22,23] Recently, it has been reported that the large enhancement of the 2PA cross section by the introduction of a butadiyne bond has also been predicted theoretically.[24] The result obtained in this study agrees with that calculation.

Effects of Monozinc Metalation and Complementary Coordination on the Enhancement of the 2PA Cross Section. As mentioned above, the expansion of π-conjugation between two porphyrins was found to be one of the important reasons for the enhancement of the 2PA cross section. When considering the relationship between molecular structure and 2PA properties, it is interesting to examine further the effect of the complementary coordination of imidazolyl to zinc and the monozinc metalation that induces the molecular polarization. For this reason, we examined the 2PA properties of the bisporphyrin units of monozinc complex **7M**, biszinc complex **8M**, and bis(free base) **9** in a chloroform solution containing 3000 equiv of 1-methylimidazole. The two-photon absorption spectra of **7M**, **8M**, and **9** are shown in Figure 8. For these spectra, all sample concentrations were 0.5 mM (calculated per bisporphyrin unit). The $\sigma^{(2)}$ values for bis(free base) **9** in both the absence and the presence of 1-methylimidazole were almost the same to within

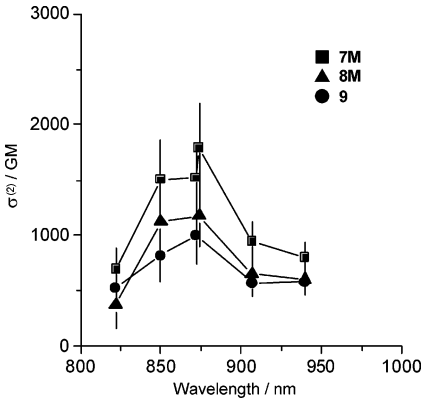

Figure 8. 2PA spectra of **7M**, **8M**, and **9** measured using femtosecond pulses in $CHCl_3$ with 1-methylimidazole (1.5 M).

the experimental error ($\sigma^{(2)} = (1.2 \pm 0.21) \times 10^3$ GM in chloroform and $(1.0 \pm 0.26) \times 10^3$ GM in chloroform with 1-methylimidazole at 873 nm), demonstrating that the presence of excess 1-methylimidazole has a negligible effect. In all the cases, the maximum $\sigma^{(2)}$ values were obtained at around 870−880 nm. The compounds **7M**, **8M**, and **9** (i.e., those without complementary coordination) also showed relatively large $\sigma^{(2)}$ values of $(1.8 \pm 0.2) \times 10^3$, $(1.2 \pm 0.14) \times 10^3$, and $(1.0 \pm 0.15) \times 10^3$ GM, respectively (Table 1). The $\sigma^{(2)}$ value of **7M** was almost twice that of the measured values for **8M** and **9**, suggesting that monozinc metalation is a positive factor for 2PA enhancement. The effect of monozinc metalation is related to molecular polarity involving intramolecular charge redistribution of the lowest unoccupied molecular orbitals (LUMOs) in the 2PA transition process (highest occupied molecular orbitals (HOMOs) and LUMOs of this and related compounds were reported in the literature[24b]) because freebase porphyrin works as an acceptor toward zinc porphyrin. However, the $\sigma^{(2)}$ value for **7M** (1.8×10^3 GM) was 4 times smaller than that for **7D** (7.6×10^3 GM), showing that the complementary coordination is another factor leading to 2PA cross section enhancement. The complementary coordination allows two-symmetric-charge redistribution in the LUMOs from the central part of the molecule to both ends, which is enhanced by the extended electronic communication through the coordination bonds. Also enhanced transition dipole moments by the excitonic coupling mechanism[25] may also contribute to the larger 2PA cross section of **7D**. These observations are also consistent with the literature.[24b]

2PA Properties of Polymer 8P. The 2PA cross section of self-assembled polymer **8P** was measured in a chloroform solution (concentration = 0.5 mM per bisporphyrin unit). Strong two-photon absorption was also observed in the Z-scan experiment for this substance. The $\sigma^{(2)}$ value per biszinc unit was estimated to be 4.0×10^3 GM at 873 nm. The enhancement factor for polymer formation is 3.3 compared with the value for monomeric biszinc complex **8M** (1.2×10^3 GM). The mean $\sigma^{(2)}$ value of polymer **8P** was estimated to be $\sim 4.4 \times 10^5$ GM, where here the number density of the molecule (N) in eq 4 was found from the M_n value of 1.5×10^5 corresponding to 110 bisporphyrin units. This value is extremely high compared with the value found for **8M**. The cross section is enhanced by a factor of 360. Even compared with the value of 7.6×10^3 GM obtained for **7D**, the result is 57 times higher. The two-photon absorption spectra for **8P** (shown in Figure 9) are similar to those for **7D**, **7M**, **8M**, and **9**. It has absorption maxima between 870 and 890 nm, suggesting that all the compounds probably go through a similar 2PA process.

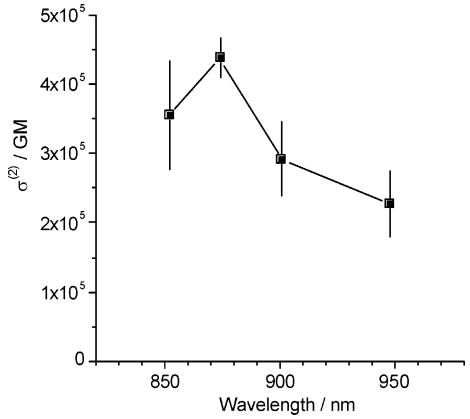

Figure 9. 2PA spectra of **8P** measured using femtosecond pulses in $CHCl_3$ with 1-methylimidazole (1.5 M).

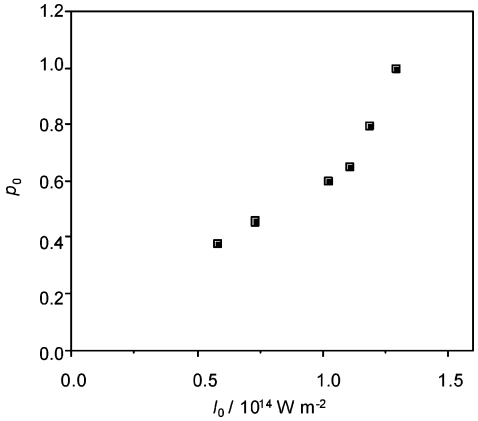

Figure 10. Plots of the two-photon absorbance q_0 versus peak intensity at the focal position I_0 for **8P** at 850 nm by using nanosecond pulses in toluene. The pulse energy ranged from 1.0 to 2.1 mJ.

Many $\sigma^{(2)}$ values have been reported to date for organic molecules including porphyrins and tetraazaporphyrins (TAPs). Most values found for organic compounds (with or without donor/acceptor groups) using femtosecond laser measurements have not exceeded 1.0×10^3 GM,[22] except in some recent reports[14a,15f,g,23] where the largest value reached 1.0×10^4 GM.[15g] Self-assembled polymer **8P** can be constructed simply by complementary coordination and exhibits the largest $\sigma^{(2)}$ values reported to date. The $\sigma^{(2)}$ value per dimer unit of **8P** ($\sim$110 dimer units) exhibits a significant increase (3.3 times) compared to that of **8M** (1 dimer unit), but it is almost the same as that of **7D** (2 dimer units), suggesting that the coupling through 3 or more dimer units slightly contributes to the enhancement of 2PA.

Nanosecond Two-Photon Absorption Properties. In general, the $\sigma^{(2)}$ value measured using nanosecond laser pulses is 2−3 orders of magnitude larger than that obtained with femtosecond pulses[21] because of the contribution of excited-state absorption (ESA) to the signal. This effect is difficult to separate from the pure 2PA signal. However, in some applications using 2PA materials (such as 2PA-PDT or the creation of 3-D optical memory devices), a laser with a nanosecond pulse may be more appropriate because of the ease of operation and availability. For this reason, we considered it important to examine the nonlinear absorption properties of the nanosecond region for **7D** and **8P**. We did a series of open Z-scan measurements with a nanosecond optical parametric oscillator pumped with a Nd:YAG laser. Figure 10 shows plots of q_0 against I_0 for **8P** at 850 nm. The pulse energy was varied between 1.0 and 2.1 mJ. The value of q_0 was almost proportional up to I_0 of 1.1×10^{14} W m^{-2}, corresponding to the incident power of 15 mW, then deviates upward. This intensity dependence exhibits that the ESA process is significant at the high-intensity region. Thus, the spectrum was measured at the lowest intensity (7.3×10^{13} W m^{-2} (1.0 mJ)), and the "effective" $\sigma^{(2)}$, which includes the contribution of ESA, was determined at the intensity by using eqs 1−4. Although the effective $\sigma^{(2)}$ varies depending on the intensity, the obtained values are a good measure of the magnitude for nanosecond applications. The obtained spectra of the effective $\sigma^{(2)}$ are shown in Figure 11. Absorption maxima were observed at 890 nm in both samples. These spectra were similar to those obtained using femtosecond measurements (Figures 8, 9, and 11). The effective $\sigma^{(2)}$ values for tetramer **7D** and polymer **8P** were calculated and were found to be 2.1×10^5 and $\sim 2.2 \times 10^7$ GM (1.1×10^5 and 2.0×10^5 GM per bisporphyrin unit), respectively. These values are 30−50 times larger than those observed in femtosecond measurements, due to the presence of an ESA contribution generated by the use of a longer pulse width. The value per bisporphyrin unit increases two times from **7D** to **8P**, although those values with femtosecond pulses are almost the same (3.8×10^3 and 4.0×10^3 GM per bisporphyrin unit for **7D** and **8P**, respectively). This suggests that the ESA process becomes more significant as the number of the repeating units increases and enhances the stepwise nonlinear absorption. The existence of such large cross sections makes the prospect of further investigation into the application of nanosecond measurements to 2PA-PDT applications well worth considering.

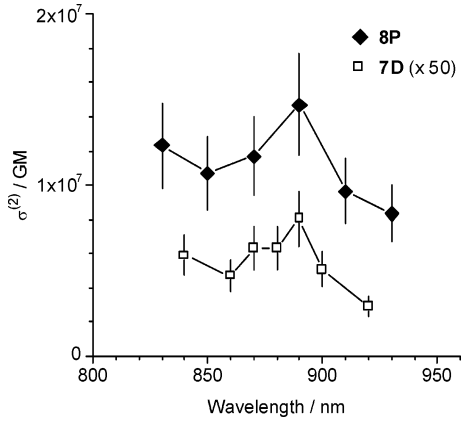

Figure 11. 2PA spectra of **7D** and **8P** measured using nanosecond pulses in toluene. The pulse energy was 1.0 mJ for all the measurements.

Three-Photon Absorption. An interesting feature of **7D** in femtosecond measurements was the parabolic behavior of the absorption cross section for wavelengths between 1188 and 1282 nm (Figure 6). This indicates a nonlinear absorption of order greater than 2. The most probable higher-order nonlinear absorption process with the femtosecond pulses is three-photon absorption (3PA). It is possible that, in fact, 2PA and 3PA occur simultaneously, especially at 1188 nm. The analysis of a model based on simultaneous 2PA and 3PA is, however, mathematically complex. As a first step, therefore, the open-aperture traces obtained for this range of wavelengths were reanalyzed and compared to a model in which only 3PA was taken into account. In this case, the normalized transmittance is described by the following equations[26a]

$$T(\zeta) = \frac{(1-R)^2\, e^{(-\alpha^{(1)}L)}}{\sqrt{\pi}p(\zeta)} \int_{-\infty}^{\infty} \ln[\sqrt{1+p(\zeta)^2\, e^{(-2x^2)}} + p(\zeta)\, e^{(-x^2)}]\, dx \quad (5)$$

$$p(\zeta) = \frac{p_0}{1 + \zeta^2} \tag{6}$$

where the parameter p_0 is defined as

$$p_0 = (2\alpha^{(3)} L'_{\text{eff}})^{1/2}(1 - R) I_0 \tag{7}$$

and $\alpha^{(3)}$ is the 3PA coefficient. L'_{eff} denotes the quadratic effective path length and is defined to be $L'_{\text{eff}} = [1 - \exp(-2\alpha^{(1)}L)]/2\alpha^{(1)}$. The p_0 was obtained by fitting eqs 5 and 6 to the measured data. For 3PA, another proportionality relation is expected between p_0 and I_0 (eq 7), and indeed, when calculated, p_0 was found to exhibit a reasonably linear relationship with I_0 (Figure 12).

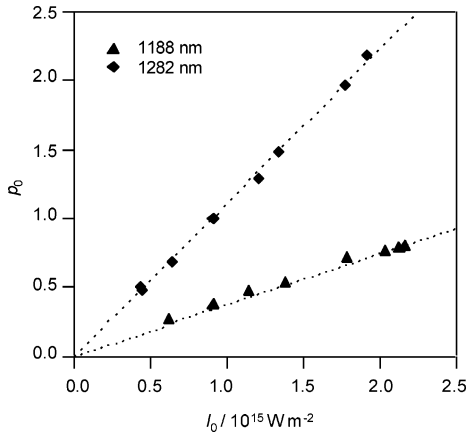

Figure 12. Plot of parameter p_0 versus on-axis peak intensity at the focal position I_0 for **7D** at different wavelengths with linear fits (dashed line). Data were obtained using femtosecond pulses.

The value of $\alpha^{(3)}$ was obtained by finding the gradient of the p_0 versus I_0 plot, and then the 3PA cross section $\sigma^{(3)}$ was found

$$\sigma^{(3)} = \frac{(h\omega)^2 \alpha^{(3)}}{N} \tag{8}$$

It should be noted here that the intrinsic 3PA process (i.e., the simultaneous absorption of three photons by the substance) is not only the process that results in a linear relationship between p_0 and I_0 such as the one observed. Stepwise 3PA (e.g., 2PA followed by an excited-state absorption process) results in the same dependence of p_0 on I_0 and should be treated as an apparent 3PA process. However, although the possibility of stepwise 3PA processes cannot be completely ruled out, we believe that the observed 3PA process originates from the intrinsic 3PA process because the intensity of the 2PA signal decreased as the incident wavelength approached the range within which the 3PA behavior was observed (1188−1282 nm), and furthermore this wavelength range corresponds to 3 times the wavelength of the strong Soret band.

On the basis of the analysis above, the 3PA cross sections were estimated to be 7.1×10^{-89} and 1.8×10^{-89} m^6 s^2 at 1188 and 1282 nm, respectively. Although these values are relatively small in comparison with the reported values for organic compounds (10^{-92}−10^{-79} m^6 s^2),[26] to our best knowledge this is the first observation of the 3PA process in porphyrin compounds. Materials exhibiting 3PA as a dominant nonlinear process may be interesting for further high-resolution 3-D optical memory and PDT applications, which could thus make use of even longer-wavelength NIR light.

Conclusions

We have synthesized butadiyne-linked conjugated bis(imidazolylporphyrin) **9**. The coordination dimer of its monozinc complex, **7D**, gave a large 2PA cross section value of $\sigma^{(2)} = 7.6 \times 10^3$ GM as measured using a femtosecond open-aperture Z-scan method. The expansion of porphyrin−porphyrin π-conjugation was found to be the dominant factor in this large enhancement of the $\sigma^{(2)}$ value. This was demonstrated by comparison with a meso−meso-linked porphyrin array **6D** without a butadiyne linkage. Other factors contributing to the increase in the 2PA cross section were found to be monozinc metalation and self-coordination. A simple coordination polymer **8P** obtained by the complementary coordination of meso-substituted imidazolyl to zinc also exhibited extremely strong two-photon absorption. The measured value ($\sigma^{(2)} \approx 4.4 \times 10^5$ GM at 873 nm) is the largest so far reported for organic molecules. Z-scan experiments using nanosecond pulses for **7D** and **8P** also gave huge 2PA cross section values (2.1×10^5 GM for **7D** and $\sim 2.2 \times 10^7$ GM for **8P**, respectively). The effect of ESA on these values was investigated. Finally, three-photon absorption (3PA) was observed for the first time in porphyrin compounds. The effect was seen to occur at wavelengths longer than 1180 nm.

This investigation clearly demonstrates that this method for constructing porphyrin arrays, which relies on complementary coordination of imidazolyl to zinc, is a simple and powerful tool, allowing facile modification of the molecular unit and the introduction of donor/acceptor groups that results in large $\sigma^{(2)}$ values. The enhancement of the 2PA cross section and the typically localized nature of these nonlinear effects makes the production and investigation of self-assembled porphyrin arrays such as the one presented here of considerable interest for future 2PA-PDT applications.

Experimental Section

The synthesis of compound **6D** was reported previously.[13c] ^{1}H and ^{13}C NMR spectra were measured by using a JEOL ECP 600 spectrometer. MALDI-TOF mass spectra were recorded with a Voyager DE-STR (PerSeptive Biosystems). Dithranol was used as a matrix. Gel permeation chromatography (GPC) was performed using a Hewlett-Packard 1100 series chromatograph with a JAIGEL 4H-A column (exclusion limit 5×10^5 Da, Japan Analytical Industry Co. Ltd.). The molecular weight and polydispersity were estimated relative to monodisperse polystyrene standards.[27]

Synthesis of 5,15-Bis(*n*-heptyl)-10-(trimethylsilylpropagyl)-20-(1-methyl-2-imidazolyl) Porphyrin: 13. Under a nitrogen atmosphere, 1-methyl-2-formyl-imidazole (**10**) (4.1 mmol), *n*-heptyldipyrromethane (**11**) (4.1 mmol), and trimethylsilylpropynal (**12**) (2 mmol) were dissolved in 1 L of chloroform. Trifluoroacetic acid (TFA, 8.6 mmol) was added. After the solution was stirred for 4 h at room temperature, 2,3,5,6-tetrachloro-*p*-benzoquinone (chloranil, 6.5 mmol) was added, and the reaction solution was stirred for a further 3 h. The reaction mixture was washed with aqueous sodium bicarbonate, and then the organic layer was evaporated. The crude product was purified using silica gel column chromatography (eluent chloroform/acetone = 9:1) with a yield of 0.08 mmol (4.0%). MS (MALDI-TOF) found for $[M]^+$ 682.4173, calcd 682.4179. λ_{abs} (chloroform): 427, 528, 567, 608, 667 nm. λ_{em} ($\lambda_{\text{ex}} = 427$ nm, chloroform): 670, 741 nm. ^{1}H NMR (600 MHz, $CDCl_3$, δ): −2.71 (s, 2H, inner proton), 0.52 (s, 9H, $Si(CH_3)_3$), 0.73 (t, $J = 7$ Hz, 6H, CH_3), 1.14−1.16 (m, 8H, CH_2), 1.29−1.34 (m, 4H, CH_2), 1.54 (quintet, 4H, CH_2), 2.20−2.22 (m, 4H, CH_2), 3.12 (s, 3H, NCH_3), 4.40−448 (m, 4H, CH_2), 7.30 (s, 1H, im), 7.57 (s, 1H, im), 8.20 (br, 2H, b), 8.91 (br, 2H, b), 9.16 (d, $J =$ 4 Hz, 2H, b), 9.55 (d, $J = 4$ Hz, 2H, b). ^{13}C NMR (150 MHz,

$CDCl_3$, δ): 0.50 ($Si(CH_3)_3$), 14.2 (CH_2), 22.8 (CH_2), 29.4 (CH_2), 30.5 (CH_2), 32.0 (CH_2), 34.6 (NCH_3), 34.9 (CH_2), 38.7 (CH_2), 100.0 (TMS−C≡CEnDash−), 102.2 (meso), 107.5 (TMS−C≡C−), 114.8 (meso), 119.1 (meso), 121.4 (im), 126.3 (im), 127−131 (br, 4 carbons (Porβ1−4)), 144−148 (br, 4 carbons (α1−4)), 148.2 (im); the other 4 carbons (Porα) could not be observed by broadening.

Synthesis of 5,15-Bis(*n*-heptyl)-10-(trimethylsilylpropagyl)-20-(1-methyl-2-imidazolyl) Porphyrinatozinc: 13Zn. To a solution of free base porphyrin **13** (0.059 mmol) in 12 mL of chloroform was added 3 mL of a saturated solution of zinc acetate dihydrate in methanol. After the solution was stirred for 1 h at room temperature, the reaction solution was washed with water and evaporated (quantitatively). MS (MALDI-TOF) found for $[M]^+$ 744.3311, calcd 744.3314. λ_{abs} (chloroform): 425, 444, 577, 642 nm. λ_{em} (λ_{ex} = 444 nm, chloroform): 645, 704 nm. ^{1}H NMR (600 MHz, $CDCl_3$, δ): 0.73 (s, 9H, $Si(CH_3)_3$), 1.00 (t, J = 7 Hz, 6H, CH_3), 1.44−2.49 (m, 4H, CH_2), 1.50−1.57 (m, 4H, CH_2), 1.65 (s, 3H, NCH_3), 1.94−1.99 (m, 2H, CH_2), 2.04 (d, J = 2 Hz, 1H, im), 2.00−2.07 (m, 2H, CH_2), 2.70−2.74 (m, 2H, CH_2), 2.85−2.89 (m, 2H, CH_2), 4.96−5.09 (m, 4H, CH_2), 5.38 (d, J = 4 Hz, 2H, Porβ), 5.47 (d, J = 2 Hz, 1H, im), 8.81 (d, J = 4 Hz, 2H, Porβ), 9.61 (d, J = 4 Hz, 2H, Porβ), 9.91 (d, J = 4 Hz, 2H, Porβ). ^{13}C NMR (150 MHz, $CDCl_3$, δ): 0.7 ($Si(CH_3)_3$), 14.3 (CH_2), 22.9 (CH_2), 29.8 (CH_2), 31.0 (CH_2), 32.3 (CH_2), 32.7 (NCH_3), 35.9 (CH_2), 39.5 (CH_2), 98.4 (meso), 99.0 (TMS−C≡C−), 99.7 (TMS−C≡C−), 109.7 (meso), 117.9 (im), 118.9 (meso), 121.4 (im), 127.3 (Porβ4), 129.0 (Porβ1), 129.3 (Porβ3), 131.3 (Porβ2), 145.5 (im), 147.4 (Porα), 150.2 (Porα), 150.8 (Porα), 151.6 (Porα).

Synthesis of 5,15-Bis(*n*-heptyl)-10-ethynyl-20-(1-methyl-2-imidazolyl) Porphyrinatozinc: 14. Under a nitrogen atmosphere, a 1 M THF solution of tetrabutylammonium fluoride (0.18 mL, 0.18 mmol) was added to a solution of porphyrin **13Zn** (0.059 mmol) in 5 mL of chloroform. After being stirred for 1 h at room temperature, the reaction solution was washed with water and evaporated (quantitatively). λ_{abs} (chloroform): 422, 440, 576, 636 nm. λ_{em} (λ_{ex} = 440 nm, chloroform): 640, 698 nm.

Synthesis of 1,3-Bis(5 -(15-(1-methyl-2-imidazolyl)-10,20-bis(*n*-heptyl)-porphyrinyl))butadiyne: 9. To a solution of **14** (0.27 mmol) in pyridine (20 mL) was added CuCl (18.9 mmol) under O_2 bubbling. After being stirred for 2 h at room temperature, the mixture was washed with 25% aqueous ammonia and then extracted with $CHCl_3$. The organic layer was evaporated under reduced pressure. The crude product of zinc complex polymer **8P** was dissolved in 10 mL of $CHCl_3$, and *p*-toluenesulfonic acid monohydrate (2.7 mmol) was added to the solution to demetalate once for purification. After the solution was stirred for 1 h at room temperature, aqueous $NaHCO_3$ solution was added. The organic layer was evaporated under reduced pressure. The residue was purified through a silica gel column eluting with $CHCl_3$/MeOH (10:1) and GPC to afford pure **9** (15%). MS (high-resolution MALDI-TOF) found for $[M]^+$ 1218.7413, calcd 1218.7411. λ_{abs} (chloroform): 444, 475, 607, 714 nm. λ_{em} (λ_{ex} = 444 nm, chloroform): 721, 800 nm. ^{1}H NMR (600 MHz, $CDCl_3$, δ): −2.12 (s, 2H, inner proton), 0.88 (t, J = 7 Hz, 12H, CH_3), 1.22−1.43 (m, 16H, CH_2), 1.56 (m, 8H, CH_2), 1.81 (m, 8H, CH_2), 2.54 (m, 8H, CH_2), 3.44 (s, 6H, NCH_3), 4.94 (m, 8H, CH_2), 7.49 (s, 2H, im), 7.70 (s, 2H, im), 8.76 (d, J = 4 Hz, 4H, β), 9.40 (d, J = 4 Hz, 4H, β), 9.58 (d, J = 4 Hz, 4H, β), 10.03 (d, J = 4 Hz, 4H, β).

Preparation of Biszinc Complex 7. To a solution of **9** (0.05 mmol) in 5 mL of chloroform was added 1 mL of a saturated solution of zinc acetate dihydrate in methanol. After being stirred for 1 h at room temperature, the reaction solution was washed with water and evaporated (quantitatively). MS (high-resolution MALDI-TOF) found for $[M]^+$ 1344.5648, calcd 1344.5650. λ_{abs} (chloroform): 430, 461, 500, 577, 676, 741 nm.

Preparation of Self-Assembly 7D. To a solution of free base bisporphyrin **9** (4 μmol) in 2 mL of chloroform was added 0.5 mL of zinc acetate methanol solution (4 μmol). After being stirred for 1 h at room temperature, the reaction solution was washed with water and evaporated. The residue was purified through GPC eluting with $CHCl_3$ to afford pure **5D**. MS (high-resolution MALDI-TOF) found for $[M]^+$ 1280.6549, calcd 1280.6546. λ_{abs} (chloroform): 429, 455, 484, 583, 660, 732 nm. λ_{em} (λ_{ex} = 484 nm, chloroform): 749, 840 nm.

Preparation of Monomeric Species in Solution. Since the complementary coordination of imidazolyl to zinc can be dissociated by adding a competing ligand,[13b,d] 1-methylimidazole was titrated into 0.5 mM (calculated per monomeric form) solution of polymer **8P** in chloroform (0.5 mL). The change in the absorption spectra was saturated after the addition of 3000 equiv of 1-methylimidazole, indicating complete dissociation to monomer **8M**. This condition was employed for the 2PA measurements of **7M**, **8M**, and **9** (for the control experiment).

Measurement of Nonlinear Absorption. Femtosecond 2PA spectra were measured from 820 to 1280 nm using the open-aperture Z-scan method[20] with an optical parametric amplifier (SpectraPhysics OPA-800) operating at 1 kHz and pumped by a Ti:sapphire regenerative amplifier system (Spectra-Physics Spitfire, Merlin, Tsunami, and Millennia). The pulse width (typically 120 fs) and spatial profile of the incident pulses were characterized by autocorrelation and knife-edge measurements, respectively. The incident pulses can be regarded as Gaussian in time and space. The optical setup used for the Z-scan measurements is the same as those described elsewhere.[14] The on-axis peak intensity of the incident pulses at the focal point I_0 were in the range (0.2−2.2) × 10^{15} W m^{-2}. The pulse repetition rate was 10 Hz, reduced from 1 kHz by the use of mechanical choppers. The sample solution in $CHCl_3$, poured in a 1 mm quartz cuvette, was used for the measurements. Nanosecond measurements were performed by using an optical parametric oscillator (Continuum Surelight OPO) pumped with a third harmonic generation beam from a Q-switched Nd:YAG laser (Continuum Surelight I-10). The pulse width and the repetition rate were 5 ns and 10 Hz, respectively. The pulse energy was adjusted to 1.0 mJ for all measurements, and a 1 mm quartz cuvette was also used. The laser beam was focused using a plano-convex lens (f = 100 mm) with a beam waist of around 0.035 mm at the focal point. The pulse energy of 1.0 mJ in this setup corresponds to the I_0 of 7.3 × 10^{13} W m^{-2}. The Z-scan measurement was performed for rhodamine B in a methanol solution, and the cross section value was found to be 21 GM at 1064 nm, which was almost consistent with the reported value of 14.3 GM measured by the fluorescence method at 1064 nm.[28] Because the porphyrin sample in $CHCl_3$ tended to decompose due to the high intensity of the irradiation from the nanosecond pulse at the focal point, toluene was used as the solvent.

Acknowledgment. This work was supported by Grant-in-Aids for Scientific Research (No. 15205020), Exploratory Research (No. 16655072), and Scientific Research on Priority Areas (No. 16033244, Reaction Control of Dynamic Complexes) from the Ministry of Education, Culture, Sports, Science and Technology, Japan (Monbu Kagakusho).

Supporting Information Available: ^{1}H NMR, MALDI-TOF MS, and GPC data for key compounds. This material is available free of charge via the Internet at http://pubs.acs.org.

References and Notes

(1) (a) Bhawalkar, J. D.; Kumar, N. D.; Zhao, C. F.; Prasad. P. N. *J. Clin. Laser Med. Surg.* **1997**, *15*, 201. (b) Wachter, E. A.; Partridge, W. P.; Fisher, W. G.; Dees, H. C.; Petersen, M. G. *Proc. SPIE−Int. Soc. Opt. Eng.* **1998**, *3269*, 68. (c) Liu, J.; Zhao, Y. W.; Zhao, J. Q.; Xia, A. D.; Jiang, L. J.; Wu, S.; Ma, L.; Dong, Y. Q.; Gu, Y. H. *J. Photochem. Photobiol., B* **2002**, *68*, 156.

(2) (a) Parthenopoulos, D. A.; Rentzepis, P. M. *Science* **1989**, *245*, 843. (b) Strickler, J. H.; Webb, W. W. *Opt. Lett.* **1991**, *16*, 1780. Dvornikov, A. S.; Rentzepis, P. M. *Opt. Commun.* **1995**, *119*, 341. (c) Shen, Y.; Friend, C. S.; Jiang, Y.; Jakubczyk, D.; Swiatkiewicz, J.; Prasad, P. N. *J. Phys. Chem. B* **2000**, *104*, 7577. (d) Dvornikov, A. S.; Liang, Y.; Cruse, C. S.; Rentzepis, P. M. *J. Phys. Chem. B* **2004**, *108*, 8652.

(3) *Nonlinear Optics of Organic Molecules and Polymers*, Nalwa, H. S., Miyata, S., Eds.; CRC Press: Boca Raton, FL 1997.

(4) (a) Kawata, S.; Sun, H.-B.; Tanaka, T.; Takada, K. *Nature* **2001**, *412*, 697. (b) Zhou, W.; Kuebler, S. M.; Braun, K. L.; Yu, T.; Cammack, J. K.; Ober, C. K.; Perry, J. W.; Marder, S. R. *Science* **2002**, *296*, 1106.

(5) (a) Kohler, R. H.; Cao, J.; Zipfel, W. R.; Webb, W. W. *Science* **1997**, *276*, 2039. (b) Caylor, C. L.; Dobrianov, I.; Kimmer, C.; Thorne, R. E.; Zipfel, W.; Webb, W. W. *Phys. Rev. E* **1999**, *59*, R3831. (c) Miller, M. J.; Wei, S. H.; Parker, I.; Cahalan, M. D. *Science* **2002**, *296*, 1869.

(6) Kershaw, S. In *Characterization Techniques and Tabulations for Organic Nonlinear Optical Materials*; Kuzyk, M. G., Dirk, C. W., Eds.; Marcel Dekker: New York, 1998; Chapter 7.

(7) Bonnett, R. *Chemical Aspects of Photodynamic Therapy*; Gordon and Breach Science Publishers: Amsterdam, 2000.

(8) *Electro-Optics Handbook*, Waynant, R. W., Ediger, M. N., Eds.; McGraw-Hill: New York, 1993; Chapter 24.

(9) (a) Gu, M.; Day, D. *Opt. Lett.* **1999**, *24*, 288. (b) Day, D.; Gu, M.; Smallridge, A. *Opt. Lett.* **1999**, *24*, 948.

(10) Albota, M.; Beljonne, D.; Brédas, J.-L.; Ehrlich, J. E.; Fu, J.-Y.; Heikal, A. A.; Hess, S. E.; Kogej, T.; Levin, M. D.; Marder, S. R.; McCord-Maughon, D.; Perry, J. W.; Röckel, H.; Rumi, M.; Subramaniam, G.; Webb, W. W.; Wu, X.-L.; Xu, C. *Science* **1998**, *281*, 1653.

(11) Reinhardt, B. A.; Brott, L. L.; Clarson, S. J.; Dillard, A. G.; Bhatt, J. C.; Kannan, R.; Yuan, L.; He, G. S.; Prasad, P. N. *Chem. Mater.* **1998**, *10*, 1863.

(12) (a) Drobizhev, M.; Karotki, A.; Kruk, M.; Rebane, A. *Chem. Phys. Lett.* **2002**, *355*, 175. (b) Drobizhev, M.; Karotki, A.; Kruk, M.; Mamardashvili, N. Zh.; Rebane, A. *Chem. Phys. Lett.* **2002**, *361*, 504. (c) Drobizhev, M.; Karotki, A.; Kruk, M.; Krivokapic, A.; Anderson, H. L.; Rebane, A. *Chem. Phys. Lett.* **2003**, *370*, 690. (d) Goyan, R. L.; Cramb, D. T. *Photochem. Photobiol.* **2000**, *72*, 821.

(13) (a) Kobuke, Y.; Miyaji, H. *J. Am. Chem. Soc.* **1994**, *116*, 4111. (b) Ogawa, K.; Kobuke, Y. *Angew. Chem., Int. Ed.* **2000**, *39*, 4070. (c) Ogawa, K.; Zhang, T.; Yoshihara, K.; Kobuke, Y. *J. Am. Chem. Soc.* **2002**, *124*, 22. (d) Kobuke, Y.; Ogawa, K. *Bull. Chem. Soc. Jpn.* **2003**, *76*, 689. (e) Ogawa, K.; Ohashi, A.; Kobuke, Y.; Kamada, K.; Ohta, K. *J. Am. Chem. Soc.* **2003**, *125*, 13356. (f) Hwang, I.-W.; Park, M.; Ahn, T. K.; Yoon, Z. S.; Ko, D. M.; Kim, D.; Ito, F.; Ishibashi, Y.; Khan, S. R.; Nagasawa, Y.; Miyasaka, H.; Ikeda, C.; Takahashi, R.; Ogawa, K.; Satake, A.; Kobuke, Y. *Chem.−Eur. J.* **2005**, in press.

(14) (a) Kamada, K.; Ohta, K.; Iwase, Y.; Kondo, K. *Chem. Phys. Lett.* **2003**, *372*, 386. (b) Iwase, Y.; Kondo, K.; Kamada, K.; Ohta, K. *J. Mater. Chem.* **2003**, *13*, 1573. (c) Audebert, P.; Kamada, K.; Matsunaga, K.; Ohta. K. *Chem. Phys. Lett.* **2003**, *367*, 62. (d) Antonov, L.; Kamada, K.; Ohta, K.; Kamounah, S. *Phys. Chem. Chem. Phys.* **2003**, *5*, 1193. (e) Kamada, K.; Matsunaga, K.; Yoshino, A.; Ohta, K. *J. Opt. Soc. Am. B* **2003**, *20*, 529.

(15) (a) Piet, J. J.; Warman, J. M.; Anderson, H. L. *Chem. Phys. Lett.* **1997**, *266*, 70. (b) Anderson, H. L. *Inorg. Chem.* **1994**, *33*, 972. (c) Anderson, H. L. *Chem. Commun.* **1999**, 2323. (d) Thorne, J. R. G.; Kuebler, S. M.; Denning, R. G.; Blake, I. M.; Taylor, P. N.; Anderson, H. L. *Chem. Phys.* **1999**, *248*, 181. (e) Screen, T. E. O.; Thorne, J. R. G.; Denning, R. G.; Bucknall, D. G.; Anderson, H. L. *J. Am. Chem. Soc.* **2002**, *124*, 9712. (f) Karotki, A.; Drobizhev, M.; Dzenis, Y.; Taylor, P. N.; Anderson, H. L.; Rebane, A. *Phys. Chem. Chem. Phys.* **2004**, *6*, 7. (g) Drobizhev, M.; Stepanenko, Y.; Dzenis, Y.; Karotki, A.; Rebane, A.; Taylor, P. N.; Anderson, H. L. *J. Am. Chem. Soc.* **2004**, *126*, 15352.

(16) (a) Lin, V. S.-Y.; DiMagno, S. G.; Therien, M. J. *Science* **1994**, *264*, 1105. (b) Lin, V. S.-Y.; Therien, M. J. *Chem.−Eur. J.* **1995**, *1*, 645. (c) Angiolillo, P. J.; Uyeda, H. T.; Duncan, T. V.; Therien, M. J. *J. Phys. Chem. B* **2004**, *108*, 11893.

(17) Tomohiro, Y.; Satake, A.; Kobuke, Y. *J. Org. Chem.* **2001**, *66*, 8442.

(18) Cameron, M.; Bennett, G. *J. Org. Chem.* **1957**, *22*, 557.

(19) (a) Osuka, A.; Shimidzu, H. *Angew. Chem., Int. Ed. Engl.* **1997**, *36*, 135. (b) Nakano, A.; Osuka, A.; Yamazaki, I.; Yamazaki, T.; Nishimura, Y. *Angew. Chem., Int. Ed.* **1998**, *37*, 3023. (c) Aratani, N.; Osuka, A. *Bull. Chem. Soc. Jpn.* **2001**, *74*, 1361.

(20) Sheik-Bahae, M.; Said, A. A.; Wei, T.-H.; Hagan, D. G.; van Stryland, E. W. *IEEE J. Quantum Electron.* **1990**, *26*, 760.

(21) (a) Swiatkiewicz, J.; Prasad, P. N.; Reinhardt, B. A. *Opt. Commun.* **1998**, *157*, 135. (b) Kim, O.-K.; Lee, K.-S.; Woo, H. Y.; Kim, K.-S.; He, G. S.; Swiatkiewicz, J.; Prasad, P. N. *Chem. Mater.* **2000**, *12*, 284. (c) Lei, H.; Wang, H. Z.; Wei, Z. C.; Tang, X. J.; Wu, L. Z.; Tung, C. H.; Zhou, G. Y. *Chem. Phys. Lett.* **2001**, *333*, 387.

(22) (a) Abbotto, A.; Beverina, L.; Bozio, R.; Facchetti, A.; Ferrante, C.; Pagani, G. A.; Pedron, D.; Signorini, R. *Org. Lett.* **2002**, *4*, 1495. (b) Kim, O. K.; Lee, K. S.; Woo, H. Y.; Kim, K. S.; He, G. S.; Swiatkiewicz, J.; Prasad, P. N. *Chem. Mater.* **2001**, *13*, 4071. (c) Chung, S. J.; Kim, K. S.; Lin, T. C.; He, G. S.; Swiatkiewicz, J.; Prasad, P. N. *J. Phys. Chem. B* **1999**, *103*, 10741.

(23) (a) Abbotto, A.; Beverina, L.; Bozio, R.; Facchetti, A.; Ferrante, C.; Pagani, G. A.; Pedronb, D.; Signorini, R. *Chem. Commun.* **2003**, 2144. (b) Belfield, K. D.; Liu, Y.; Negres, R. A.; Fan, M.; Pan, G.; Hagan, D. J.; Hernandez, F. E. *Chem. Mater.* **2002**, *14*, 3663 (c) Porrès, L.; Mongin, O.; Katan, C.; Charlot, M.; Pons, T.; Mertz, J.; Blanchard-Desce, M. *Org. Lett.* **2004**, *6*, 47.

(24) (a) Zhou, X.; Ren, A.-M.; Feng, J.-K.; Liu, X.-J.; Zhang, Y.-D. *ChemPhysChem* **2003**, *4*, 991. (b) Zhou, X.; Ren, A.-M.; Feng, J.-K. *Chem.−Eur. J.* **2004**, *10*, 5623.

(25) McRae, E. G.; Kasha, M. *J. Chem. Phys.* **1958**, *28*, 721.

(26) (a) Tykwinski, R. R.; Kamada, K.; Bykowski, D.; Hegmann, F. A.; Hinkle, R. J. *J. Opt. A: Pure Appl. Opt.* **2002**, *4*, S202. (b) Wang, X. M.; Zhou, G. Y.; Wang, D.; Wang, C.; Fang, Q.; Jiang, M. H. *Bull. Chem. Soc. Jpn.* **2001**, *74*, 1977. (c) He, G. S.; Bhawalkar, J. D.; Prasad, P. N.; Reinhardt, B. A. *Opt. Lett.* **1995**, 1524. (d) Bhawalkar, J. D.; He, G. S.; Prasad, P. N. *Opt. Commun.* **1995**, 587. (e) Zhang, J. X.; Cui, Y. P.; Wang, M. L.; Xu, C. X.; Zhong, Y.; Liu, J. Z. *Chem. Lett.* **2001**, 824. (f) Drobizhev, M.; Karotki, A.; Kruk, M.; Dzenis, Y.; Rebane, A.; Suo, Z.; Spangler, C. W. *J. Phys. Chem. B* **2004**, *108*, 4221.

(27) See for example, Balke, S. T.; Hamielec, A. E.; LeClair, B. P.; Pearce, S. L. *Ind. Eng. Chem. Prod. Res. Dev.* **1969**, *8*, 54.

(28) Hermann, J. P.; Ducuing, J. *Opt. Commun.* **1972**, *6*, 101.